Stepwise evolution and exceptional conservation of ORF1a/b overlap in coronaviruses

Han Mei and Anton Nekrutenko

Department of Biochemistry and Molecular Biology, The Pennsylvania State University, University Park, PA, USA

Correspondence should be addressed to AN

The programmed frameshift element (PFE) rerouting translation from *ORF1a* to *ORF1b* is essential for propagation of coronaviruses. A combination of genomic features that make up PFE—the overlap between the two reading frames, a slippery sequence, as well as an ensemble of complex secondary structure elements—puts severe constraints on this region as most possible nucleotide substitution may disrupt one or more of these elements. The vast amount of SARS-CoV-2 sequencing data generated within the past year provides an opportunity to assess evolutionary dynamics of PFE in great detail. Here we performed a comparative analysis of all available coronaviral genomic data available to date. We show that the overlap between *ORF1a* and *b* evolved as a set of discrete 7, 16, 22, 25, and 31 nucleotide stretches with a well defined phylogenetic specificity. We further examined sequencing data from over 350,000 complete genomes and 55,000 raw read datasets to demonstrate exceptional conservation of the PFE region.

Coronaviruses have large 26-32 kbp +-strand RNA genomes. The initial ⅔ of the genome is occupied by an open reading frame (ORF) *ORF1ab* encoding nsps essential for coronaviral life cycle. As the designation "ab" suggests it contains two reading frames with the 3'-end of *ORF1a* overlapping with the 5'-terminus of *ORF1b*. *ORF1b* is in -1 phase relative to ORF1a and translated via the -1 programmed ribosomal frameshifting controlled by the programmed frameshift element (PFE). As *ORF1b* encodes crucial components of coronavirus transcription/replication machinery including the RNA-dependent RNA polymerase (RdRp) disrupting PFE abolishes viral replication completely (Brierley 1995; Plant et al. 2010; Sola et al. 2015; Kelly et al. 2020). PFE consists of three consecutive elements: (1) an attenuator loop, (2) the “NNN WWW H” slippery heptamer, and (3) a pseudoknot structure (Kelly et al. 2020; Huston et al. 2021). The sequence and structural conformation of these elements determines the efficiency of the frameshift event, which ranges from 15 to 30% in SARS-CoV and SARS-CoV-2 (Baranov et al. 2005; Kelly et al. 2020). Because disruption of FSE arrests viral replication it is a promising therapeutic target. As a result a number of recent studies have scrutinized its characteristics (reviewed in (Rangan et al. 2021)) revealing a fluid secondary structure (Iserman et al. 2020; Ziv et al. 2020; Huston et al. 2021). In addition to secondary structures FSE harbors the overlap between *ORF1a* and *ORF1b*. It is defined as the stretch of sequence from "H" in the slippery heptamer to the stop codon of *ORF1a*. The position of *ORF1a* stop codon determines overlap length. For example, in SARS-CoV-2 it is 16 bp while in mouse hepatitis virus (MHV) it is 23 nt (Plant et al. 2010).

Our group has been interested in the evolutionary dynamics of overlapping coding regions (Nekrutenko et al. 2005; Chung et al. 2007; Szklarczyk et al. 2007). The vast amount of newly generated sequence and functional data—a result of the current SARS-CoV-2/COVID-19 pandemic—provides an opportunity to reexamine our current knowledge. The length of the *ORF1a* and *ORF1b* overlap is phylogenetically conserved. It evolved in a stepwise manner, where the changes in the overlap length are results of the loss of *ORF1a* stop codons leading to *ORF1a* extension, and the acquisition of insertions and deletions causing early stops of ORF1a.

Distance-based methods had shown that the δ-coronavirus genus was an early split-off lineage compared to α-, β-, and γ-coronavirus (Fig. 1). Comparisons of the RdRp, 3CL^{pro}, HEL, M, and N proteins suggested that γ- was more closely related to δ-coronavirus, while α- and β-coronavirus cluster together forming a distant clade (de Groot et al. 2012; Lau et al. 2012; Woo et al. 2012; Coronaviridae Study Group of the International Committee on Taxonomy of Viruses 2020). However, comparing the S protein trees, α- and δ-coronavirus share a higher amino acid identity, while β- and γ-coronavirus cluster together (Lau et al. 2012). Due to this we initially assumed that α, β, and γ form an unresolved trifurcation (Fig. 1). To assess all possible configurations within this region we surveyed all genomic sequences of family Coronaviridae available from the National Center for Biotechnology Information (NCBI; see Methods). The distribution of overlap lengths among 4,904 coronaviral genomes (Table S1) is shown in Fig. 2. There are five distinct overlap length groups (7, 16, 22, 25, and 31 nt) with clear taxonomic specificity.

We then compared the first 15 amino acids of *ORF1b* in all 4,904 entries (Fig. 3). The amino acid sequences are highly conserved: positions 1 (R), 2 (V), 4 (G), 7 (S), 11-13 (ARL), and 15 (P) are almost invariable and highly redundant. Next, we compared underlying nucleotide sequences of the PFE region (Fig. 4). This suggests the following potential series of events. δ-coronavirus with 7 nt overlap most likely represents the ancestral state. Comparing coronaviruses with 7 nt (δ-coronavirus) and 31 nt (α- and γ-coronavirus) in the overlap, the stop codon to generate a 7 nt overlap is abolished at positions 5–7, through substitution events, which extends ORF1a to the next available stop codon at positions 38–40. This extension results in a new overlap with 31 nt in length (Fig. 4A). Comparing coronaviruses with 31 nt (α- and γ-coronavirus) and 25 nt (β-coronavirus: Nobecovirus) overlaps reveals a "GTA" insertion at positions 28–30. "TA" from the "GTA" together with the following "G" forms a new stop codon leading to a 31 → 25 nt shortening of the overlap. In a Nobecovirus with a 25 nt overlap, the 31 nt overlap stop codon (at positions 38–40) is still observable (Fig. 4B). Further comparison of coronaviruses with 31 nt (α- and γ-coronavirus) and 22 nt (β-coronavirus: Embecovirus and Merbecovirus) overlaps revealed a "GTA" insertion as well, but at positions 22–24. "TA" at positions 23–24 and the following "A" or "G" at position 25 constitute a new stop codon. In the 22 nt overlap, substitutions have been observed at the original stop codon (at positions 38–40) from 31 nt overlap coronaviruses; more specifically, "C" appears at position 39 (Fig. 4C). Finally, we compared coronaviruses with 31 and 16 nt length in the overlap. The same "GTA" insertion footprint was found, at positions 16–18 ahead of the two "GTA" insertions in 31 → 25 nt and 31 → 22 nt events. "TA" at positions 17–18 and the following "A" at position 19 form the stop codon in the 16 nt overlap coronaviruses. In addition, deletions at positions 13–15 were observed (Fig. 4D). These deletions are referred as "TCT"-like, since "TCT" are the dominant nucleotides observed at positions 13–15 in the 7 and 31 nt overlap coronaviruses. At positions 38–40, the ancestral stop codon in the 31 nt overlap coronaviruses can not be seen, since the nucleotide at position 39 is invariably represented by "T" (Fig. 4D). The variable position of the stop codon likely has an implication to the frameshift efficiency in these taxa as was shown by Bhatt et al. (Bhatt et al. 2021). These authors demonstrated that extension of the distance between the slippery heptamer and the stop codon of 0-frame decreases frameshifting frequency: an increase in the distance by 15 nucleotides, as is the case in α- and γ-coronaviruses (Fig. 4), decreases frameshifting by ~20%, while removal of the stop decreases it by half.

The abundance of SARS-CoV-2 sequencing data allows examining the substitution dynamics that may be present in population- and individual-level sequencing data. For population-level analysis we identified variants in the PFS region from >350,000 complete genome sequences available from GISAID (see Methods). However, because GISAID contains only assembled genomes, this data does not provide information about individual-level (intrasample) variation. For this we performed a detailed analysis of >55,000 samples generated with the COG-UK (Lythgoe et al. 2021) consortium (see (Maier et al. 2021) for analysis details). A summary of results from both analyses is shown in Table 1. There is little variation in the FSE region as the fraction of samples containing individual substitutions appears to be small (the two “Count” columns in Table 1). In addition, the vast majority of substitutions (30 out of 36 marked in Table 1) may be an artifact of RNA editing events from APOBEC (Chen and MacCarthy 2017) or ADAR (Bazak et al. 2014) enzymatic complexes. The remaining six substitutions (all transitions) are predominantly located in the loop regions of the predicted FSE secondary structure (Huston et al. 2021) and thus likely have no effect on the secondary structure.

Our results provide an alternative way to assess exceptional conservation of the PFE using publicly available sequence data highlighting the fact that the entire PFE region appears to be under strong purifying selection. These patterns are similar to observations obtained from deep mutational scanning where any alteration at the majority of PFE region sites results have deleterious effects on the frameshift efficiency (e.g., (Carmody et al. 2021)).

Materials and Methods

Coronavirus entries retrieval and filter

The 35,152 coronaviral entries in the NCBI taxonomy database were sorted by length, and only those larger than 14,945 nt were kept, leaving a total of 4,939 genomes. The slippery site and following overlap sequences were manually inspected, in case that the slippery site was incorrectly annotated. We further filtered out those entries if they contain no annotation information, or have gapped sequences in the overlap. By applying these filters, we finally had 4,904 coronavirus entries (Table S1), of which the overlap could be unambiguously determined.

Amino acid alignment and nucleotide alignment of the overlap region

For all *δ-coronavirus* entries in Table S1, the first 13 amino acids of ORF1b were taken to generate a consensus sequence using WebLogo (Crooks et al. 2004). The same was done to *Alphacoronavirus* and *γ-coronavirus*. Within *β-coronavirus*, for *Nobecovirus*, *Embecovirus*, and *Merbecovirus*, the first 14 amino acids were used to build the consensus; for *Hibecovirus* and *Sarbecovirus*, the first 13 amino acids were used. In terms of the nucleotide sequence alignments, for each genus/subgenus, the nucleotide sequences used to generate the amino acids mentioned above were taken to make the nucleotide consensus sequence using WebLogo.

Processing of GISAID data

Each genome was subjected to codon-aware alignment with the NCBI reference genome (accession number NC_045512) and then subdivided into ten regions based on CDS features: ORF1a (including nsp10), ORF1b (starting with nsp12), S, ORF3a, E, M, ORF6, ORF7a, ORF8, N, and ORF10. For each region, we scanned and discarded sequences containing too many ambiguous nucleotides to remove data with too many sequencing errors. Thresholds were 0.5% for the S gene, 0.1% for ORF1a and ORF1b genes, and 1% for all other genes. We mapped individual sequences to the NCBI reference genome (NC_045512) using a codon-aware extension to the Smith-Waterman algorithm implemented in HyPhy (Pond et al. 2005; Gianella et al. 2011) translated mapped sequence to amino-acids, and performed multiple protein sequence alignment with the auto settings function of MAFFT (version 7.453) (Katoh and Standley 2013). Codon sequences were next mapped onto the amino-acid alignment. Variants were called directly.

Acknowledgements

The authors are grateful to Sergei Kosakovsky Pond for providing variant data from GISAID sequences. This work is funded by NIH Grants U41 HG006620 and NSF ABI Grant 1661497. The funders had no role in study design, data collection and analysis, decision to publish, or preparation of the manuscript.

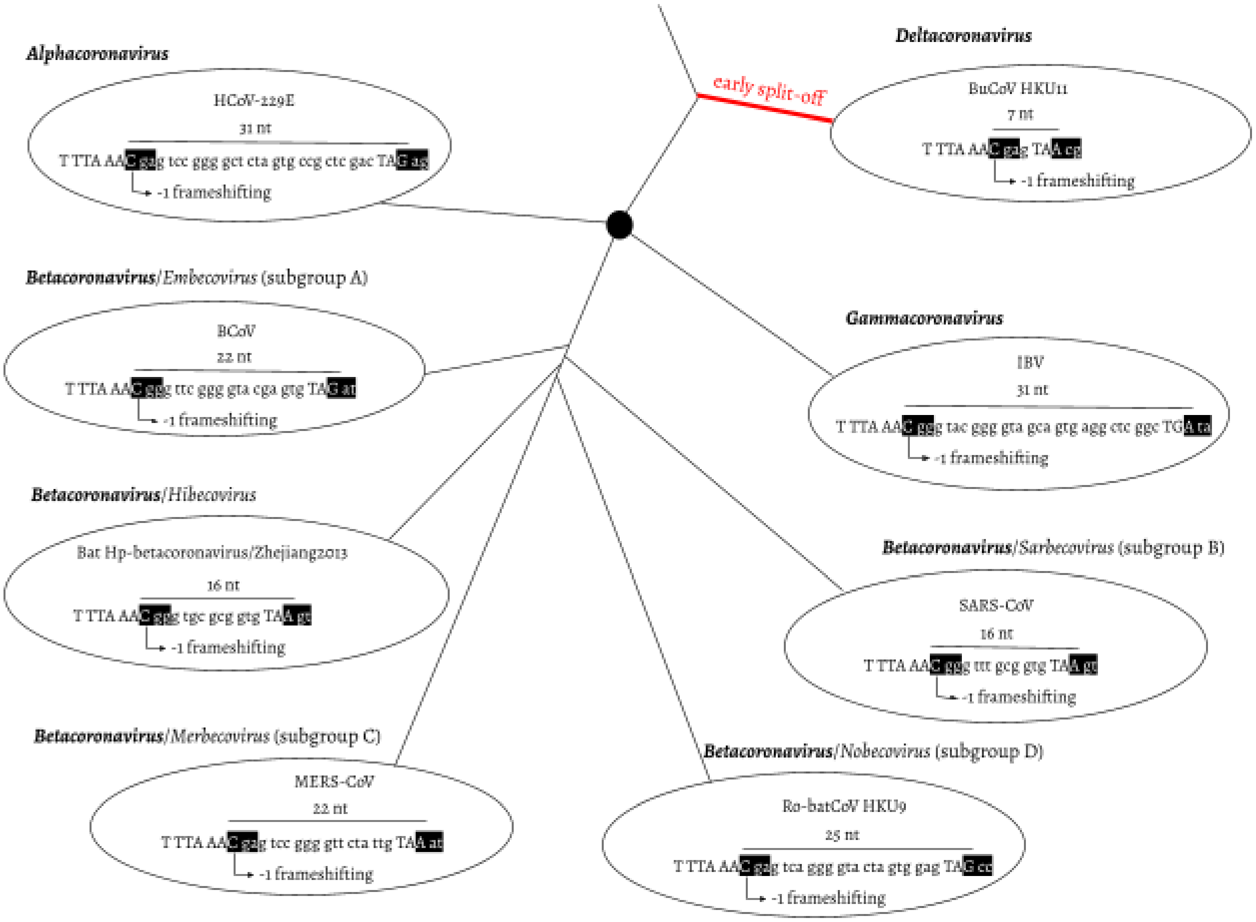
Alphacoronavirus
HCoV-229E
31 nt
T TTA AAC ggg tcc ggg gct cta gtg ccg ctc gac TAG ag
-1 frameshifting
early split-off
Deltacoronavirus
BuCoV HKU11
7 nt
T TTA AAC ggg TAA cg
-1 frameshifting
Betacoronavirus/Embecovirus (subgroup A)
BCoV
22 nt
T TTA AAC ggg ttc ggg gta cga gtg TAG at
-1 frameshifting
Gammacoronavirus
IBV
31 nt
T TTA AAC ggg tac ggg gta gca gtg agg ctc ggc TGA ta
-1 frameshifting
Betacoronavirus/Hibecovirus
Bat Hp-betacoronavirus/Zhejiang2013
16 nt
T TTA AAC ggg tgc gcg gtg TAA gt
-1 frameshifting
Betacoronavirus/Sarbecovirus (subgroup B)
SARS-CoV
16 nt
T TTA AAC ggg ttt gcg gtg TAA gt
-1 frameshifting
Betacoronavirus/Merbecovirus (subgroup C)
MERS-CoV
22 nt
T TTA AAC ggg tcc ggg gtt cta ttg TAA at
-1 frameshifting
Betacoronavirus/Nobecovirus (subgroup D)
Ro-batCoV HKU9
25 nt
T TTA AAC ggg tca ggg gta cta gtg gag TAG cc
-1 frameshifting

Fig. 1. Overlap between ORF1a and b as a phylogenetic character. ORF1a frame 0 is shown as three consecutive nucleotides separated by spaces. The slippery site "TTT AAA C" and the ORF1a stop codon are shown in upper case letters. In ORF1b frame -1, two codons are shown in black boxes: the codon starting from the slippery site and the codon bypassing the ORF1a stop codon. *α-, β-*, and *γ-coronavirus* were plotted as splitting from one common node (black filled circle), with no phylogenetic order shown. HCoV-229E: Human coronavirus 229E, NC_002645.1. BCoV: Bovine coronavirus, NC_003045.1. Bat Hp-β-coronavirus/Zhejiang2013, NC_025217.1. MERS-COV, NC_019843.3. Ro-batCoV HKU9: Rousettus bat coronavirus HKU9, NC_009021.1. SARS-CoV, NC_004718.3. IBV: infectious bronchitis virus, NC_001451.1. BuCoV HKU11: Bulbul coronavirus HKU11, NC_011547.1.

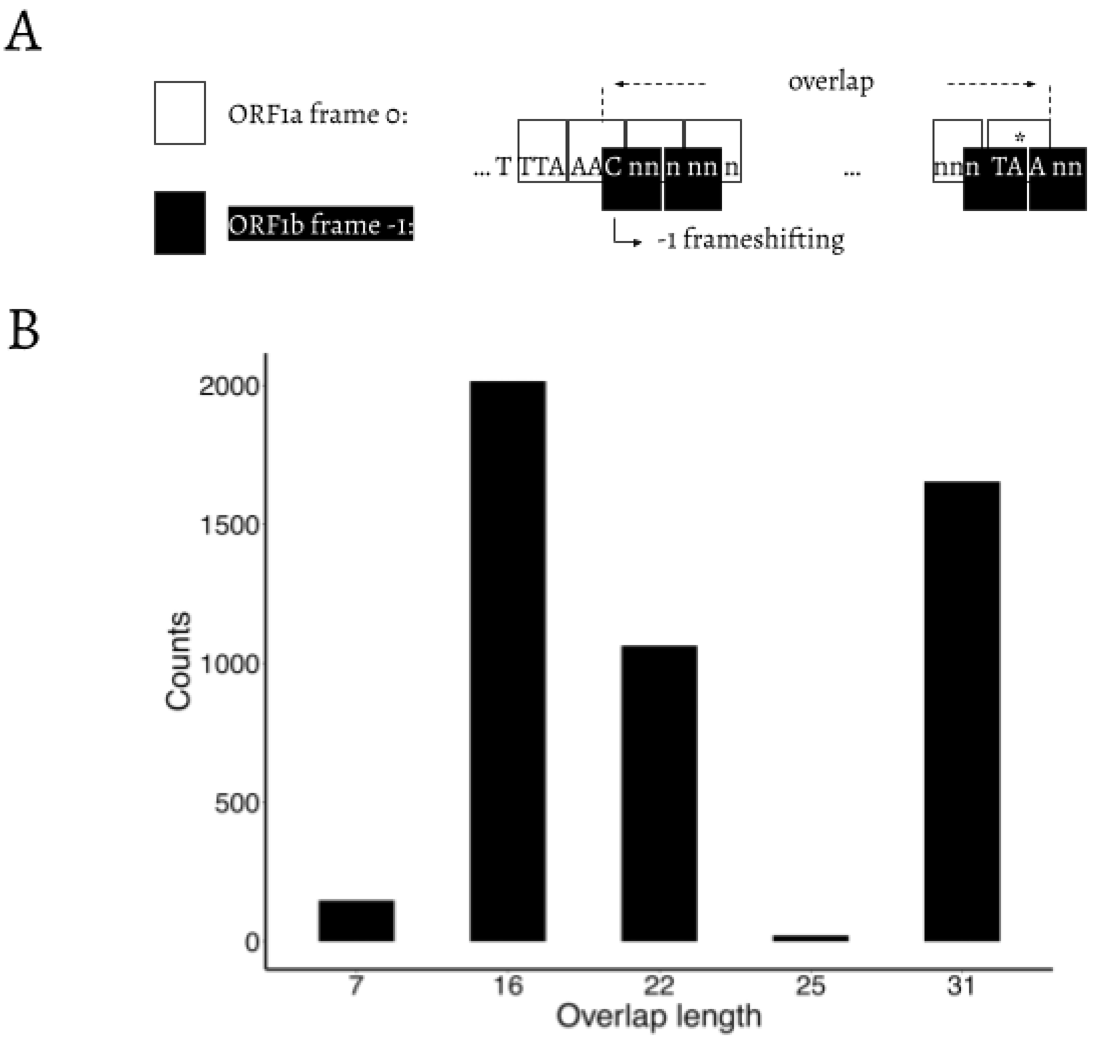

Deltacoronavirus	7 nt	148	entries
Betacoronavirus: Hibecovirus & Sarbecovirus	16 nt	2 & 2000	entries
Betacoronavirus: Embecovirus & Merbecovirus	22 nt	420 & 613	entries
Betacoronavirus: Nobecovirus	25 nt	14	entries
Alphacoronavirus & Gammacoronavirus	31 nt	1209 & 426	entries
unclassified	16 & 22 & 25 & 31 nt	71	entries

Fig. 2. A. Schematic representation of the overlap between ORF1a and ORF1b. "TTT AAA C" is the slippery site. ORF1a frame 0 is shown in white boxes. "TTT AAA C" and the ORF1a stop codon are shown in upper case letters. ORF1b frame -1 is shown in black boxes. The -1 frameshifting starts from "C" of "TTT AAA C", which is indicated at the bended arrow. * = the stop codon of ORF1a. **B.** Distribution of the length of the overlap in different genera/subgenera.

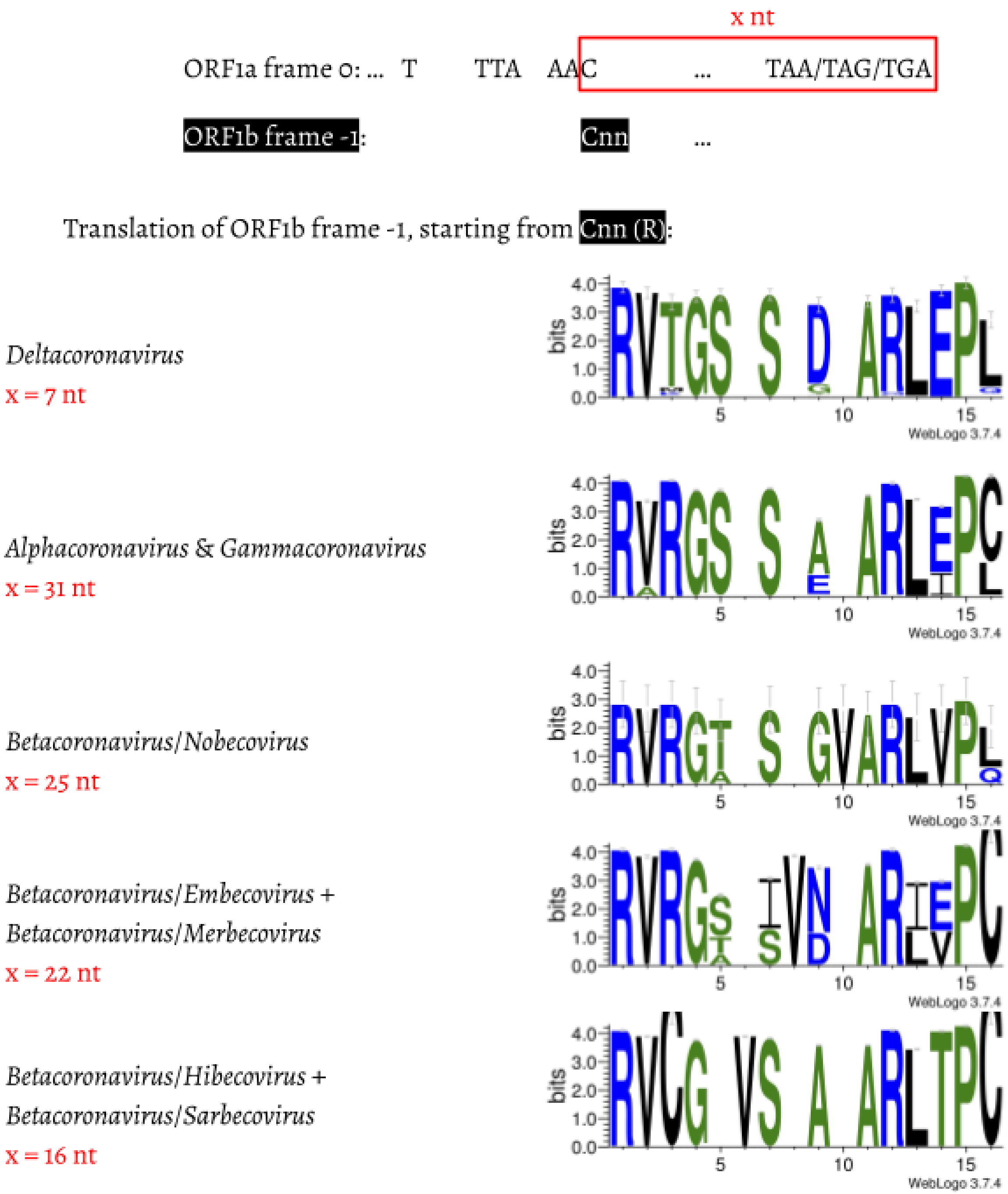
x nt
ORF1a frame 0: ... T TTA AAC ... TAA/TAG/TGA
ORF1b frame -1: Cnn ...
Translation of ORF1b frame -1, starting from Cnn (R):
Deltacoronavirus
x = 7 nt
RVTGS S D ARLEPL
Alphacoronavirus & Gammacoronavirus
x = 31 nt
RVRGS S A ARLEPC
Betacoronavirus/Nobecovirus
x = 25 nt
RVRGT S GVARLVPL
Betacoronavirus/Embecovirus +
Betacoronavirus/Merbecovirus
x = 22 nt
RVRGS IVN ARIEPC
Betacoronavirus/Hibecovirus +
Betacoronavirus/Sarbecovirus
x = 16 nt
RVCG VS A ARLTPC
bits
4.0
3.0
2.0
1.0
0.0
5
10
15
WebLogo 3.7.4

Fig. 3. Amino acid alignment of the first 13–14 amino acids in coronaviruses with different lengths in the overlap region. For each genus/subgenus shown, all coronavirus entries belonging to this group are used to generate the consensus amino acid sequences. Gaps were left to make the amino acid sequences align.

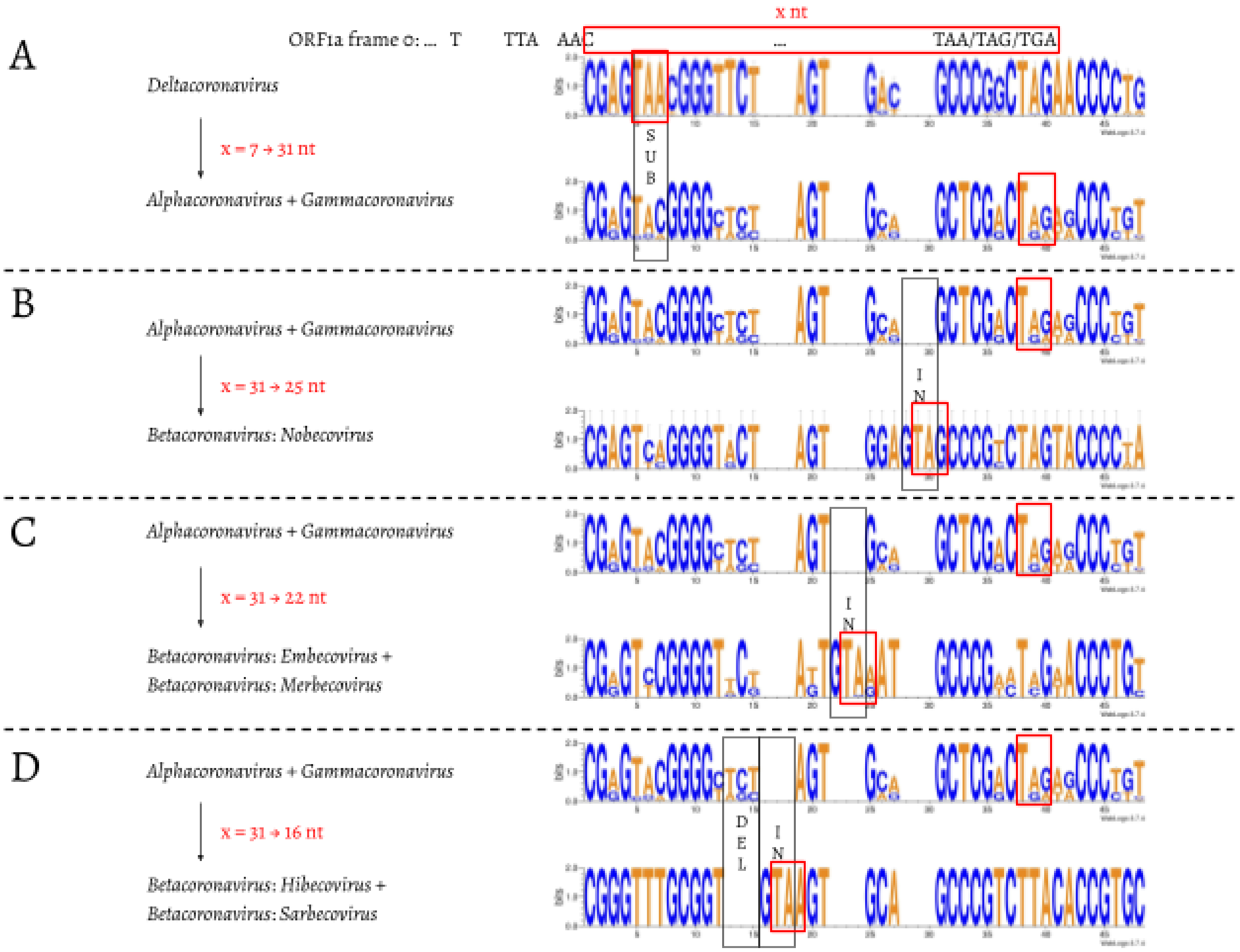
A
ORF1a frame 0: ... T TTA AAC ... TAA/TAG/TGA
x nt
Deltacoronavirus
x = 7 → 31 nt
Alphacoronavirus + Gammacoronavirus
S
U
B
B
Alphacoronavirus + Gammacoronavirus
x = 31 → 25 nt
Betacoronavirus: Nobecovirus
I
N
C
Alphacoronavirus + Gammacoronavirus
x = 31 → 22 nt
Betacoronavirus: Embecovirus +
Betacoronavirus: Merbecovirus
I
N
D
Alphacoronavirus + Gammacoronavirus
x = 31 → 16 nt
Betacoronavirus: Hibecovirus +
Betacoronavirus: Sarbecovirus
D
E
L
I
N

Fig. 4. Nucleotide alignment of the overlap in coronaviruses with 7, 31, 25, 22, and 16 nt. The footprints of substitutions, insertions, and deletions are shown in black boxes, and labelled as "SUB", "IN", and "DEL", respectively. The stop codon of ORF1a in each of the 7, 31, 25, 22, and 16 nt overlap coronaviruses is shown in a red box.

Table 1. Allelic variants within the FSE region called from complete genomes (Population) and COG-UK (Individual) data. * = potential APOBEC-edited sites; + = potential ADAR-edited sites. Site numbering is in 0-based coordinates; † = out of 355,568 complete genomes; ‡ = out of 55,163 individual samples. Location of substitutions in a stem (^{s}) or a loop (^{L}) are based on structures predicted by Huston et al. (Huston et al. 2021).

		Population		**Individual**				
Site	**Reference**	**Alternate**	**Count†**	**Alternate**	**Min AF**	**Max AF**	**Count‡**	**CoV**
*13,425	C	T	131	-	-	-	-	-
*13,429	C	T	178	-	-	-	-	-
*13,430	C	T	57	-	-	-	-	-
*13,431	C	T	18	-	-	-	-	-
+13,432	A	G	23	-	-	-	-	-
*13,434	G	A	33	-	-	-	-	-
*13,435	C	T	48	T	0.116	0.971	14	0.403
+13,437	T	C	7	C	0.985	0.988	5	0.001
^{S}13,440	G	T	6	-	-	-	-	-
*13,445	C	-	-	T	0.068	0.970	25	0.239
*13,447	G	A	6	-	-	-	-	-
*13,451	C	T	25	T	0.941	0.977	19	0.009
*13,457	C	T	251	T	0.052	0.963	19	0.842
*13,458	G	-	246	A	0.069	0.970	6	0.669
^{L}13,458	G	T	246	T	0.080	0.976	6	0.442
+13,481	A	G	9	-	-	-	-	-
*13,486	C	T	336	T	0.055	0.965	7	1.012
+13,487	A	-	-	G	0.901	0.949	12	0.017
+13,497	A	G	6	-	-	-	-	-
*13,498	C	T	16	-	-	-	-	-
*13,500	C	T	53	-	-	-	-	-
^{L}13,504	G	T	6	-	-	-	-	-
*13,505	C	T	7	T	0.887	0.917	5	0.015
^{L}13,511	A	T	13	-	-	-	-	-
^{L}13,512	G	T	13	-	-	-	-	-
*13,513	G	A	21	-	-	-	-	-
*13,514	C	T	41	T	0.065	0.889	6	0.622
*13,516	C	T	711	T	0.101	0.840	49	0.260
^{S}13,525	A	C	46	-	-	-	-	-
+13,526	T	C	14	-	-	-	-	-
+13,532	A	G	6	-	-	-	-	-
*13,535	C	T	3,999	T	0.215	0.841	23	0.223
+13,541	T	C	6	-	-	-	-	-
*13,547	C	T	59	T	0.067	0.898	8	0.373
*13,550	C	T	31	T	0.878	0.921	11	0.017

References

Baranov PV, Henderson CM, Anderson CB, Gesteland RF, Atkins JF, Howard MT. 2005. Programmed ribosomal frameshifting in decoding the SARS-CoV genome. *Virology* 332:498–510.

Bazak L, Haviv A, Barak M, Jacob-Hirsch J, Deng P, Zhang R, Isaacs FJ, Rechavi G, Li JB, Eisenberg E, et al. 2014. A-to-I RNA editing occurs at over a hundred million genomic sites, located in a majority of human genes. *Genome Res.* 24:365–376.

Bhatt PR, Scaiola A, Loughran G, Leibundgut M, Kratzel A, Meurs R, Dreos R, O'Connor KM, McMillan A, Bode JW, et al. 2021. Structural basis of ribosomal frameshifting during translation of the SARS-CoV-2 RNA genome. *Science* [Internet]. Available from: https://science.sciencemag.org/content/early/2021/05/12/science.abf3546/tab-pdf

Brierley I. 1995. Ribosomal frameshifting on viral RNAs. *Journal of General Virology* [Internet] 76:1885–1892. Available from: http://dx.doi.org/10.1099/0022-1317-76-8-1885

Carmody PJ, Zimmer MH, Kuntz CP, Harrington HR, Duckworth KE, Penn WD, Mukhopadhyay S, Miller TF, Schlebach JP. 2021. Coordination of -1 Programmed Ribosomal Frameshifting by Transcript and Nascent Chain Features Revealed by Deep Mutational Scanning. *bioRxiv* [Internet]:2021.03.11.435011. Available from: https://www.biorxiv.org/content/10.1101/2021.03.11.435011v1.abstract

Chen J, MacCarthy T. 2017. The preferred nucleotide contexts of the AID/APOBEC cytidine deaminases have differential effects when mutating retrotransposon and virus sequences compared to host genes. *PLoS Comput. Biol.* 13:e1005471.

Chung W-Y, Wadhawan S, Szklarczyk R, Pond SK, Nekrutenko A. 2007. A first look at ARFome: dual-coding genes in mammalian genomes. *PLoS Comput. Biol.* 3:e91.

Coronaviridae Study Group of the International Committee on Taxonomy of Viruses. 2020. The species Severe acute respiratory syndrome-related coronavirus: classifying 2019-nCoV and naming it SARS-CoV-2. *Nat Microbiol* 5:536–544.

Crooks GE, Hon G, Chandonia J-M, Brenner SE. 2004. WebLogo: a sequence logo generator. *Genome Res.* 14:1188–1190.

Gianella S, Delport W, Pacold ME, Young JA, Choi JY, Little SJ, Richman DD, Kosakovsky Pond SL, Smith DM. 2011. Detection of minority resistance during early HIV-1 infection: natural variation and spurious detection rather than transmission and evolution of multiple viral variants. *J. Virol.* 85:8359–8367.

de Groot RJ, Baker SC, Baric R, Enjuanes L, Gorbalenya AE, Holmes KV, Perlman S, Poon L, Rottier PJM, Talbot PJ, et al. 2012. Family coronaviridae. In: King AMQ, Lefkowitz E, Adams MJ, Carstens EB, editors. Virus taxonomy: ninth report of the International Committee on Taxonomy of Viruses. Elsevier. p. 806–828.

Huston NC, Wan H, Strine MS, de Cesaris Araujo Tavares R, Wilen CB, Pyle AM. 2021. Comprehensive in vivo secondary structure of the SARS-CoV-2 genome reveals novel regulatory motifs and mechanisms. *Mol. Cell* 81:584–598.e5.

Iserman C, Roden CA, Boerneke MA, Sealfon RSG, McLaughlin GA, Jungreis I, Fritch EJ, Hou YJ, Ekena J, Weidmann CA, et al. 2020. Genomic RNA Elements Drive Phase Separation of the SARS-CoV-2 Nucleocapsid. *Mol. Cell* 80:1078–1091.e6.

Katoh K, Standley DM. 2013. MAFFT multiple sequence alignment software version 7: improvements in performance and usability. *Mol. Biol. Evol.* 30:772–780.

Kelly JA, Olson AN, Neupane K, Munshi S, San Emeterio J, Pollack L, Woodside MT, Dinman JD. 2020. Structural and functional conservation of the programmed −1 ribosomal frameshift signal of SARS coronavirus 2 (SARS-CoV-2). *J. Biol. Chem.* [Internet]. Available from: http://www.jbc.org/content/early/2020/06/22/jbc.AC120.013449.abstract

Lau SKP, Woo PCY, Yip CCY, Fan RYY, Huang Y, Wang M, Guo R, Lam CSF, Tsang AKL, Lai KKY, et al. 2012. Isolation and characterization of a novel Betacoronavirus subgroup A coronavirus, rabbit coronavirus HKU14, from domestic rabbits. *J. Virol.* 86:5481–5496.

Lythgoe KA, Hall M, Ferretti L, de Cesare M, MacIntyre-Cockett G, Trebes A, Andersson M, Otecko N, Wise EL, Moore N, et al. 2021. SARS-CoV-2 within-host diversity and transmission. *Science* [Internet]. Available from: https://science.sciencemag.org/content/early/2021/03/09/science.abg0821

Maier W, Bray S, van den Beek M, Bouvier D, Coraor N, Miladi M, Singh B, De Argila JR, Baker D, Roach N, et al. 2021. Freely accessible ready to use global infrastructure for SARS-CoV-2 monitoring. *bioRxiv* [Internet]. Available from: http://dx.doi.org/10.1101/2021.03.25.437046

Nekrutenko A, Wadhawan S, Goetting-Minesky P, Makova KD. 2005. Oscillating evolution of a mammalian locus with overlapping reading frames: an XLalphas/ALEX relay. *PLoS Genet.* 1:e18.

Plant EP, Rakauskaite R, Taylor DR, Dinman JD. 2010. Achieving a golden mean: mechanisms by which coronaviruses ensure synthesis of the correct stoichiometric ratios of viral proteins. *J. Virol.* 84:4330–4340.

Pond SL, Frost SD, Muse SV. 2005. HyPhy: hypothesis testing using phylogenies. *Bioinformatics* 21:676–679.

Rangan R, Watkins AM, Chacon J, Kretsch R, Kladwang W, Zheludev IN, Townley J, Rynge M, Thain G, Das R. 2021. De novo 3D models of SARS-CoV-2 RNA elements from consensus experimental secondary structures. *Nucleic Acids Res.* 49:3092–3108.

Sola I, Almazán F, Zúñiga S, Enjuanes L. 2015. Continuous and Discontinuous RNA Synthesis in Coronaviruses. *Annu Rev Virol* 2:265–288.

Szklarczyk R, Heringa J, Pond SK, Nekrutenko A. 2007. Rapid asymmetric evolution of a dual-coding tumor suppressor INK4a/ARF locus contradicts its function. *Proceedings of the National Academy of Sciences* [Internet] 104:12807–12812. Available from: http://dx.doi.org/10.1073/pnas.0703238104

Woo PCY, Lau SKP, Lam CSF, Lau CCY, Tsang AKL, Lau JHN, Bai R, Teng JLL, Tsang CCC, Wang M, et al. 2012. Discovery of seven novel Mammalian and avian coronaviruses in the genus deltacoronavirus supports bat coronaviruses as the gene source of alphacoronavirus and betacoronavirus and avian coronaviruses as the gene source of gammacoronavirus and deltacoronavirus. *J. Virol.* 86:3995–4008.

Ziv O, Price J, Shalamova L, Kamenova T, Goodfellow I, Weber F, Miska EA. 2020. The Short- and Long-Range RNA-RNA Interactome of SARS-CoV-2. *Mol. Cell* 80:1067–1077.e5.